PERGAMON

Available online at www.sciencedirect.com

SCIENCE DIRECT®

Polyhedron 22 (2003) 83–92

POLYHEDRON

www.elsevier.com/locate/poly

Structural and spectral characterization of transition metal complexes of 2-pyridineformamide *N*(4)-dimethylthiosemicarbazone

Larissa M. Fostiak [a], Isabel García [b], John K. Swearingen [a], Elena Bermejo [b], Alfonso Castiñeiras [b,*], Douglas X. West [c]

[a] *Department of Chemistry, Illinois State University, Normal, IL 61790-4160, USA*
[b] *Departamento de Química Inorgánica, Facultad de Farmacia, Universidad de Santiago de Compostela, E-15706 Santiago de Compostela, Spain*
[c] *Department of Chemistry, 351700, University of Washington, Seattle, WA 98125-1700, USA*

Received 9 July 2002; accepted 30 August 2002

Abstract

Sodium in dry methanol reduces 2-cyanopyridine in the presence of *N*(4)-dimethylthiosemicarbazide to produce 2-pyridineformamide *N*(4)-dimethylthiosemicarbazone, HAm4DM. Complexes with iron(III), cobalt(III), nickel(II), copper(II), palladium(II) and platinum(II) have been prepared and characterized by spectroscopic techniques. In addition, the crystal structures of [Ni(Am4DM)(OAc)], [Ni(Am4DM)(CH_3CN)]ClO_4, [Cu(Am4DM)(OAc)] and [Pt(Am4DM)(DMSO)]$Cl\cdot 2H_2O$ are included. Coordination of the anionic thiosemicarbazone ligand is via the pyridyl nitrogen, imine nitrogen and thiolato sulfur atoms. The acetato groups in [Ni(Am4DM)(OAc)] and [Cu(Am4DM)(OAc)] are coordinated as monodentate ligands by one oxygen and the other oxygen interacts intermolecularly with the amide NH_2 function of Am4DM. Coordination of the DMSO molecule in [Pt(Am4DM)(DMSO)]$Cl\cdot 2H_2O$ is through sulfur to give an essentially planar cation.
© 2002 Elsevier Science Ltd. All rights reserved.

Keywords: Iron(III); Cobalt(II); Nickel(II); Copper(II); Palladium(II); Platinum(II); Spectral properties; Crystal structures; 2-Pyridineformamide; *N*(4)-dimethylthiosemicarbazone complexes

1. Introduction

Although 2-formyl-, 2-acetyl-, and 2-benzoylpyridine N(4)-substituted thiosemicarbazones and their metal complexes [1–3] have substantial in vitro activity against various human tumor lines [4], their lack of aqueous solubility causes poor results for in vivo testing. In order to enhance water solubility, a new series of N(4)-substituted thiosemicarbazones has been prepared in which the thiosemicarbazone moiety is attached to an amide carbon rather than an aldehyde or ketone carbon. Previously, we have communicated our studies of metal complexes of 2-pyridineformamide thiosemicarbazone [5,6], 2-pyridineformamide *N*(4)-methylthiosemicarbazone [7,8], 2-pyridineformamide 3-piperidylthiosemicarbazone [9,10] and 2-pyrdineformamide 3-hexamethyleneiminylthiosemicarbazone [11]. Recently, we communicated the spectral and structural properties of 2-pyridineformamide *N*(4)-dimethyl-thiosemicarbazone, HAm4DM, Fig. 1, and its Group XII metal complexes [12]. Here we report on the syntheses and spectroscopic studies of transition metal complexes of HAm4DM. Crystal structures of [Ni(Am4DM)(OAc)], [Ni(Am4DM)(CH_3CN)]ClO_4, [Cu(Am4DM)(OAc)] and [Pt(Am4DM)(DMSO)]$Cl\cdot 2H_2O$ are included.

2. Experimental

2.1. Physical measurements

Elemental analyses for C, H, N, and S were performed on a Carlo Erba EA model 1108 elemental analyser. Melting points (m.p.) were determined in open tubes with a Büchi apparatus and are uncorrected. IR spectra were obtained with Nicolet 5SXC and Magna

* Corresponding author. Tel.: +34-981-594-636; fax: +34-981-547-163
E-mail address: qiac01@usc.es (A. Castiñeiras).

0277-5387/02/$ - see front matter © 2002 Elsevier Science Ltd. All rights reserved.
PII: S0277-5387(02)01330-X

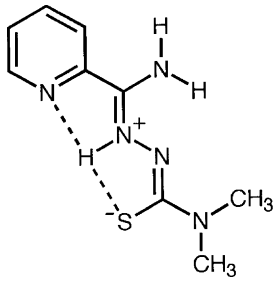

Fig. 1. Depiction of bifurcated 2-pyridineformamide *N*(4)-dimethylthiosemicarbazone, HAm4DM.

850 FT-IR spectrometers using KBr pellets or Nujol mulls between CsI plates. Electronic spectra were acquired as Nujol mulls impregnated on filter paper with a Cary 5E spectrometer. The magnetic susceptibilities were measured with a Johnson Mattey magnetic susceptibility balance. EPR spectra were obtained in 3 mm pyrex tubes with a Bruker EMX spectrometer using a conventional insert Dewar at liquid nitrogen temperature. ^{1}H and ^{13}C NMR spectra in DMSO-d_6 were run in Bruker AMX 300 and WM 300 instruments, respectively, using TMS as internal reference. ^{195}Pt NMR spectrum was run on a Bruker AMX 500 apparatus in dimethylformamide with D_2O as reference. Mass spectra (FAB, 3-nitrobenzyl alcohol, Xe, 8 kV) were obtained in a Kratos MS 50 apparatus equipped with a DS-90 data acquisition system. Electron impact ionization (70 eV) was effected using the direct sample insertion system with the lower feasible sample temperature.

2.2. Materials

All the chemicals (Aldrich) were of reagent grade and unless otherwise specified, were used as received. The solvents were purified using conventional methods. 2-Cyanopyridine was purchased from Aldrich and used as received, and *N*(4)-dimethylthiosemicarbazide was prepared as described by Scovill [13].

2.2.1. Caution

Although we have not encountered any problems, it should be kept in mind that perchlorate salts of metal complexes are potentially explosive and should be handled with care.

2.2.2. Preparation of the ligand

Following the literature procedure for the reduction of 2-cyanopyridine [14], sodium (0.092 g, 4 mmol) was added to 25 ml of MeOH, which had been dried over $CaSO_4$, and the solution stirred until complete dissolution occurred. 2-Cyanopyridine (2.6 g, 25 mmol) was then added, and the mixture stirred for 1/2 h, and *N*(4)-dimethylthiosemicarbazide (2.98 g, 25 mmol) was added in small portions over a period of 1/2 h. On addition of another 20 ml of MeOH the mixture was gently refluxed for a minimum of 4 h. Slow evaporation of MeOH produced the 2-pyridineformamide *N*(4)-dimethylthiosemicarbazone, HAm4DM.

HAm4DM: Yellow; (1.580 g, 25.0%): m.p. (°C) 155. MS (IE): *m*/*z*, *RA*(%) = 223(15) M^+. *Anal*. Found: C, 48.4; H, 5.9; N, 31.2; S, 13.6. Calc. for $C_9H_{13}N_5S$ (223.30): C, 48.4; H, 5.9; N, 31.4; S, 14.4%. IR (KBr, ν cm^{-1}): 3382s, 3219m, 3096s–3019s, (N–H), 1666s, 1601s (C=N), 1582s, 1513s [(C=N)+(C=C)], 993m (N–N), 861m (C=S), 615m (py), 394m (py). ^{1}H NMR (DMSO-d_6, δ ppm): 3.17 (3H, Me), 7.61, 8.06, 8.12, 8.74 (4H, py), 12.51 (s, a, 1H, N2H). ^{13}C NMR (DMSO-d_6, δ ppm): 38.9 (Me), 120.9 (C-4), 126.1 (C-2), 138.0 (C-3), 143.8 (C-6), 144.8 (C-5), 149.6 (C-1), 179.2 (C-7).

2.2.3. Synthesis and crystallization of the complexes

The complexes were prepared as follows: A solution of the thiosemicarbazone HAm4DM (2 or 4 mmol, as appropriate) in ethanol (30 ml) was added to a solution of the appropriate metal(II) sal (2 mmol) in 30 ml of 96% ethyl alcohol, and the mixture kept stirring for several days at room temperature (r.t. for Ni, Pd and Pt salts) or under reflux for approximately 2 h (for Fe, Co and Cu salts). The resulting solids were filtered off, washed thoroughly with cold ethanol and anhydrous ether to apparent dryness and stored in a desiccator over $CaSO_4$ until required for characterization, yields ranged from 62 to 78%. The complexes were characterized using techniques reported previously [15].

[Fe(Am4DM)$_2$](ClO$_4$): *Anal*. Found: C, 35.6; H, 3.9; N, 23.4; S, 10. 9. Calc. for $C_{18}H_{24}ClFeN_{10}O_4S_2$ (599.89): C, 36.0; H, 4.0; N, 23.4; S, 10.7%. IR (KBr, ν cm^{-1}): 3462m, 3327m (N–H), 1587s (C=N), 1500s [(C=N)+(C=C)], 1020m (N–N), 856m (C=S), 636w (py). Far-IR (Nujol, ν cm^{-1}): 407w, 389m (py), 336w (Zn–S), 279s, 258m (Zn–N), 246m, 223w (Zn–O). UV–Vis (ν cm^{-1}): 21 960, 26 000, 16 710, 15 130.

[Co(Am4DM)$_2$](ClO$_4$): *Anal*. Found: C, 35.6; H, 4.0; N, 23.0; S, 10.5. Calc. for $C_{18}H_{24}ClCoN_{10}O_4S_2$ (602.97): C, 35.9; H, 4.0; N, 23.2; S, 10.6%. IR (KBr, ν cm^{-1}): 3431m, 3314s (N–H), 1593m (C=N), 1572m, 1555s [(C=N)+(C=C)], 1016m (N–N), 846m (C=S), 621m (py). Far-IR (Nujol, ν cm^{-1}): 445w (Co–N), 381w (Co–S). UV–Vis (ν cm^{-1}): 21 960, 26 000, 16 710, 15 130.

[Ni(Am4DM)(OAc)]: MS (FAB): *m*/*z* = 340 [Ni(Am4DM)(OAc)]$^+$, 280 [Ni(Am4DM)]$^+$. *Anal*. Found: C, 38.8; H, 4.5; N, 20.5; S, 9.9. Calc. for $C_{11}H_{15}N_5NiO_2S$ (340.05): C, 38.9; H, 4.5; N, 20.6; S, 9.4%. IR (KBr, ν cm^{-1}): 3363m (N–H), 1594s (C=N), 1564s, 1537s [(C=N)+(C=C)], 1019w (N–N), 870m (C=S), 638m (py). Far-IR (Nujol, ν cm^{-1}): 480m (Ni–N), 384m (Ni–O), 369m (Ni–S). ^{1}H NMR (DMSO-d_6, δ ppm): 1.81 (s, 3H, Me–OAc), 3.20 (2, 3H, Me), 7.68, 8.07, 8.15 (4H, py), 7.40 (s, br, 2H, N5H). UV–Vis (ν cm^{-1}): 29 260, 23 620, 19 380, 16 290.

Single crystals of [Ni(Am4DM)(OAc)] suitable for analysis by X-ray diffractometry were obtained by slow evaporation of the mother liquor in air at room temperature. *Anal*. Found: C, 38.7; H, 4.4; N, 20.6; S, 9.5. Calc. for $C_{11}H_{15}N_5NiO_2S$ (340.05): C, 38.9; H, 4.5; N, 20.6; S, 9.4%.

[Ni(HAm4DM)Cl_2]: MS (FAB): $m/z = 316$ [Ni(HAm4DM)Cl]$^+$, 280 [Ni(HAm4DM)]$^+$, 633 [Ni_2(HAm4DM)$_2Cl_2$]$^+$. *Anal*. Found: C, 30.2; H, 3.5; N, 19.7; S, 9.1. Calc. for $C_9H_{13}Cl_2N_5NiS$ (352.91): C, 30.6; H, 3.7; N, 19.9; S, 9.1%. IR (KBr, ν cm^{-1}): 3281m, 3066m, 3021m (N–H), 1597s,br [(C=N)+(C=C)], 1031m (N–N), 870m (C=S), 636m (py). Far-IR (Nujol, ν cm^{-1}): 463m (Ni–N), 356m (Ni–S), 274s (Ni–Cl). Molar conductance (Ω^{-1} cm^2 mol^{-1}), 32.1 (10^{-3} M in DMF), 88 (10^{-3} M in MeOH). UV–Vis (ν cm^{-1}): 20 321, 16 949/27 933, 23 810, 21 459, 19 569 (DMF).

[Ni(HAm4DM)$_2$](ClO_4)$_2$: MS (FAB): $m/z = 280$ [Ni(HAm4DM)]$^+$, 503 [Ni(HAm4DM)$_2$]$^+$. *Anal*. Found: C, 29.8; H, 3.7; N, 18.7; S, 9.6. Calc. for $C_{18}H_{26}Cl_2N_{10}NiO_8S_2$ (704.22): C, 30.7; H, 3.7; N, 19.9; S, 9.1%. IR (KBr, ν cm^{-1}): 3447m,br, 3141m,br (N–H), 1595m (C=N), 1561s [(C=N)+(C=C)], 1089s (ClO_4^-), 1017m (N–N), 854m (C=S), 627s (ClO_4^-). Far-IR (Nujol, ν cm^{-1}): 474m (Ni–N), 364m (Ni–S). Molar conductance (Ω^{-1} cm^2 mol^{-1}), 189.9 (10^{-3} M in DMF). UV–Vis (ν cm^{-1}): 27 174, 17 241, 11 655.

Single crystals of [Ni(Am4DM)(MeCN)](ClO)$_4$ suitable for analysis by X-ray diffractometry were obtained by slow evaporation from a 1:1 (by volume) MeOH–MeCN mixture. *Anal*. Found: C, 31.2; H, 3.7; N, 11.6; S, 7.5. Calc. for $C_{11}H_{15}ClN_6NiO_4S$ (421.51): C, 31.3; H, 3.6; N, 11.7; S, 7.6%.

[Ni(HAm4DM)$_2$](NO_3)$_2$·H_2O: MS (FAB): $m/z = 280$ [Ni(HAm4DM)]$^+$, 503 [Ni(HAm4DM)$_2$]$^+$. *Anal*. Found: C, 33.2; H, 4.5; N, 25.0; S, 8.3. Calc. for $C_{18}H_{28}N_{12}N_iO_7S_2$ (647.35): C, 33.4; H, 4.4; N, 26.0; S, 9.9%. IR (KBr, ν cm^{-1}): 3350m, br, 3168m, br (N–H), 1595m (C=N), 1568m, br, [(C=N)+(C = C)], 1384s (NO_3^-), 1018m (N–N), 858w (C=S), 839w (NO_3^-), 642w (py). Far-IR (Nujol, ν cm^{-1}): 476m (Ni–N), 358m, br (Ni–S). Molar conductance (Ω^{-1} cm^2 mol^{-1}), 153.6 (10^{-3} M in DMF). UV–Vis (ν cm^{-1}): 25 253, 17 065, 11 723.

[Pd(Am4DM)Cl]: MS (FAB): $m/z = 363$ [Pd(Am4DM)Cl]$^+$, 328 [Pd(Am4DM)]$^+$, 693 [Pd_2(Am4DM)$_2$Cl]$^+$. *Anal*. Found: C, 29.3; H, 3.4; N, 18.9; S, 8.7. Calc. for $C_9H_{12}ClN_5PdS$ (363.15): C, 29.8; H, 3.3; N, 19.3; S, 8.8%. IR (KBr, ν cm^{-1}): 3439s, 3325s (N–H), 1603m (C=N), 1567m, 1537s [(C=N)+(C=C)], 1022w (N–N), 815m (C=S), 638m (py). Far-IR (Nujol, ν cm^{-1}): 484m (Pd–N), 381m (Pd–S), 344m (Pd–Cl). ^{1}H NMR (DMSO-d_6, δ ppm): 3.10 (s, 3H, Me), 7.40 (s, 2H, N5H), 7.66, 8.07, 8.21, 8.57 (4H, py). ^{13}C NMR (DMSO-d_6, δ ppm): 40.8 (C-8/C-9), 122.8 (C-4), 126.7 (C-2), 140.6 (C-3), 150.5 (C-6), 150.8 (C-5), 147.9 (C-1), 177.3 (C-7). UV–Vis (ν cm^{-1}): 28 409, 22 222, 20 576, 18 727.

[Pt(Am4DM)Cl]·H_2O: MS (FAB): $m/z = 419$ [Pt(HAm4DM)]$^+$, 869 [Pt_2(Am4DM)$_2$Cl]$^+$. *Anal*. Found: C, 22.5; H, 2.6; N, 14.3; S, 6.7. Calc. for $C_9H_{14}ClN_5OPtS$ (470.85): C, 23.0; H, 3.0; N, 14.9; S, 6.8%. IR (KBr, ν cm^{-1}): 3453m, 3324m (N–H), 1605m (C=N), 1572s, 1521sh [(C=N)+(C=C)], 1059m (N–N), 840w (C=S), 616m (py). Far-IR (Nujol, ν cm^{-1}): 461m (Pt–N), 395m (Pt–S), 333m (Pt–Cl). ^{1}H NMR (DMSO-d_6, δ ppm): 3.18 (s, 3H, Me), 7.37 (s, 2H, N5H), 7.68, 7.99, 8.23, 8.80 (4H, py). ^{13}C NMR (DMSO-d_6, δ ppm): 40.6 (C-8/C-9), 123.6 (C-4), 127.7 (C-2), 140.1 (C-3), 151.9 (C-6), 153.8 (C-5), 146.1 (C-1), 176.8 (C-7). UV–Vis (ν cm^{-1}): 28 902, 22 831, 19 960, 18 416.

Single crystals of [Pt(Am4DM)(DMSO)]Cl·$2H_2O$ suitable for analysis by X-ray diffractometry were obtained by slow evaporation of a DMSO solution in air at r.t. *Anal*. Found: C, 23.3; H, 4.0; N, 12.3; S, 11.3. Calc. for $C_{11}H_{22}ClN_5O_3PtS_2$ (567.00): C, 23.3; H, 3.9; N, 12.4; S, 11.3%.

[Cu(HAm4DM)Cl_2]: *Anal*. Found: C, 30.7; H, 3.6; N, 19.6; S, 9.1. Calc. for $C_9H_{13}Cl_2CuN_5S$ (357.74): C, 30.2; H, 3.7; N, 19.6; S, 9.0%. IR (KBr, ν cm^{-1}): 3407s, 3346m, 3298m, 3252s (N–H), 1591m (C=N), 1560s [(C=N)+(C=C)], 1014m (N–N), 851m (C=S), 624m (py). Far-IR (Nujol, ν cm^{-1}): 455w (Cu–N), 369m (Cu–S), 320m (Cu–Cl). UV–Vis (ν cm^{-1}):19 400, 14 980.

[Cu(Am4DM)Cl]: *Anal*. Found: C, 33.4; H, 3.5; N, 21.0; S, 10.0. Calc. for $C_9H_{12}ClCuN_5S$ (321.29): C, 33.6; H, 3.8; N, 21.4; S, 10.0%. IR (KBr, ν cm^{-1}): 3421m, 3224s (N–H), 1590s (C=N), 1556s [(C=N)+(C=C)], 1013m (N–N), 849w (C=S), 627m (py). Far-IR (Nujol, ν cm^{-1}): 460m (Cu–N), 365w (Cu–S), 308m (Cu–Cl). UV–Vis (ν cm^{-1}): 16 460.

[Cu(Am4DM)(OAc)]: *Anal*. Found: C, 38.5; H, 4.6; N, 21.0; S, 9.5. Calc. for $C_{11}H_{15}CuO_2N_5S$ (344.88): C, 38.3; H, 4.4; N, 20.6; S, 9.3%. IR (KBr, ν cm^{-1}): 3228m (N–H), 1581m (C=N), 1559s [(C=N)+(C=C)], 1011m (N–N), 864m (C=S), 619w (py). Far-IR (Nujol, ν cm^{-1}): 439m (Cu–N), 365w (Cu–S). UV–Vis (ν cm^{-1}): 16 770

Single crystals of [Cu(Am4DM)(OAc)] suitable for analysis by X-ray diffractometry were obtained by slow evaporation of the mother liquor in air at r.t. *Anal*. Found: C, 38.3; H, 4.5; N, 20.5; S, 9.3. Calc. for $C_{11}H_{15}CuO_2N_5S$ (344.88): C, 38.3; H, 4.4; N, 20.6; S, 9.3%.

2.3. X-ray data collection and reduction

Crystals of [Ni(Am4DM)(OAc)], [Ni(Am4DM)-(CH_3CN)]ClO_4, [Cu(Am4DM)(OAc)] and [Pt-(Am4DM)(DMSO)]Cl·$2H_2O$, were mounted on glass fibers and used for data collection at 293 K. Cell constants and an orientation matrix for data collection

were obtained by least-squares refinement of the diffraction data from 25 reflections in the range of $9.58^\circ < \theta < 11.69^\circ$ for [Ni(Am4DM)(OAc)], $9.13^\circ < \theta < 24.13^\circ$ for [Ni(Am4DM)(CH_3CN)]ClO_4, $3.69^\circ < \theta < 15.67^\circ$ for [Cu(Am4DM)(OAc)] and $10.25^\circ < \theta < 20.85^\circ$ for [Pt(Am4DM)(DMSO)]$Cl\cdot 2H_2O$. Data was acquired for [Ni(Am4DM)(CH_3CN)]ClO_4 with an Enraf–Nonius CAD4 automatic diffractometer (Cu Kα, $\lambda = 1.54184$ Å) and the other three crystals with a Nonius MACH3 automatic diffractometer (Mo K$\alpha = 0.71073$ Å). The ω–scan technique was used and the data were corrected for Lorentz and polarization effects [16]. The structures were solved by Patterson and Fourier methods [17], were refined on F^2 by a full-matrix least-squares procedure using anisotropic displacement parameters [18] and an absorption correction (ψ–scans) was applied. Hydrogen atoms on carbon and nitrogen for [Ni(Am4DM)(CH_3CN)]ClO_4 and [Pt(Am4DM)(DMSO)]$Cl\cdot 2H_2O$ were located in their calculated positions (C–H = 0.93–0.97 Å, N–H = 0.86 Å) and were refined using a riding model. The H atoms in the other two complexes and H atoms of the water molecules were located in difference Fourier maps and were refined isotropically. Atomic scattering factors are from International Tables for Crystallography [19], and molecular graphics are from PLATON [20]. A summary of the crystal data, experimental details and refinement results are listed in Table 1.

3. Results and discussion

3.1. Crystal structures description

All the four complexes of formula [Ni(Am4DM)(OAc)], [Ni(Am4DM)(CH_3CN)]ClO_4, [Cu(Am4DM)(OAc)] and [Pt(Am4DM)(DMSO)]$Cl\cdot 2H_2O$ are four-coordinate and have a square-planar geometry. The bond distances for the four complexes are given in Table 2 and their bond angles in Table 3. Table 4 lists the hydrogen bonding interactions and Table 5 the mean plane data and angles between planes. Figs. 2–5 show the perspective views.

3.1.1. Structure of [Ni(Am4DM)OAc]

The crystal structure, Fig. 2, shows anionic Am4DM coordinated in the expected NNS tridentate fashion and a monodentate acetato ligand, which is the same stoichiometry found for [Ni(Am4M)(OAc)], [Ni(Ampip)(OAc)] and [Ni(Amhexim)(OAc)], where Am4M, Ampip and Amhexim are the anions of 2-pyridineformamide *N*(4)-methyl-thiosemicarbazone [7], 2-pyridineformamide 3-piperidylthiosemicarbazone [9] and 2-pyridineformamide 3-hexamethyleneiminylthiosemicarbazone [11], respectively. The metal–ligand and the thiosemicarbazone bond distances in [Ni(Am4DM)(OAc)] are within similar to the distances found for the aforementioned nickel(II) complexes indicating that the N(4)-substituent has little effect on the coordination to nickel(II) by these amide thiosemicarbazones. Compared with HAm4DM [12], [Ni(Am4DM)(OAc)] has a longer S(1)–C(17) bond, 1.752(4) Å compared with 1.723(3) Å, and a marginally shorter N(13)–C(17) bond, 1.319(5) Å compared with 1.337(3) Å, but C(16)–N(12) is unchanged on coordination. These differences are less than would be found for the analogous thiosemicarbazones of 2-formyl- [1] and 2-benzoylpyridine [3] because HAm4DM, like its 2-acetypyridine analogue, is in the bifurcated *E′* conformation, Fig. 1. The bond angles about the nickel(II) center and within the thiosemicarbazone moiety are essentially the same as found for the previously studied nickel acetato complexes [7,9,11] except for Ni(1)–O(11)–C(11). Most likely due to packing effects ∠ Ni(1)–O(11)–C(11) is 118.9(3)° for [Ni(Am4DM)(OAc)] compared with 121.4(3)° and 116.7(4)° for [Ni(Ampip)(OAc)] and [Ni(Amhexim)(OAc)], respectively. The three complexes are in different crystal systems and have different numbers of molecules in the unit cell (i.e. [Ni(Am4DM)(OAc)], $Z = 16$; [Ni(Ampip)(OAc)], $Z = 2$ and [Ni(Amhexim)(OAc)], $Z = 4$) probably resulting in different spatial requirements for the N(4)-function.

The strongest hydrogen bonding interaction for [Ni(Am4DM)(OAc)], [Ni(Ampip)(OAc)] and [Ni(Amhexim)(OAc)] involves a $N(15)H_2$ hydrogen, H(15)B, interacting with the non-coordinated oxygen atom of the acetato group, O(12), in a neighboring molecule. The H(15B)ΛO(12) distance is approximately 2.1 Å in these three nickel(II) complexes, but the non-bonding N(15)–H(15B)···O(12) distance varies as follows: [Ni(Am4DM)(OAc)], 2.800(4) Å; [Ni(Ampip)(OAc)], 2.836(5) Å and [Ni(Amhexim)(OAc)], 2.889(7) Å, due to increased spatial requirements of the N4 azacyclic rings. The four donor atoms, N(11)–N(12)–S(1)–O(11), in [Ni(Am4DM)(OAc)] are nearly planar and nickel(II) is 0.019 (2) Å from the plane similar to the distances found for other nickel acetato complexes of 2-pyridineformamide N(4)-substituted thiosemicarbazones [7,9,11]. The acetato function makes an angle of approximately 77° with coordination plane compared with approximately 80.5° for [Ni(Ampip)(OAc]) [9].

3.1.2. Structure of [Ni(Am4DM)(CH_3CN)]ClO_4

Preparations with $Ni(ClO_4)_2$ often lead to a product with the stoichiometry found with HAm4M, octahedral $[Ni(HAm4M)_2](ClO_4)_2$ [7]. Similarly, $[Ni(HAm4DM)_2](ClO_4)_2$ is formed, but surprisingly, 4-coordinate, planar [Ni(Am4DM)(CH_3CN)]ClO_4 crystallized from a 1:1 (by volume) CH_3OH–CH_3CN mixture. Thus, it is interesting to compare [Ni(Am4DM)(CH_3CN)]ClO_4 with [Ni(Am4DM)(OAc)] to see how coordination of Am4DM is affected by an

Table 1
Crystal data and structure refinement for [Ni(Am4DM)(OAc)], [Ni(Am4DM)(CH_3CN)]ClO_4, [Cu(Am4DM)(OAc)] and [Pt(Am4DM)(DMSO)]$Cl\cdot 2H_2O$

Empirical formula	$C_{11}H_{15}N_5NiO_2S$	$C_{11}H_{15}ClN_6NiO_4S$	$C_{11}H_{15}CuN_5O_2S$	$C_{11}H_{22}ClN_5O_3PtS_2$
Color; Habit	Brown, prism	Brown, plate	Green, prism	Orange, plate
Formula weight	340.05	421.51	344.88	567.00
Crystal size (mm)	$0.35 \times 0.30 \times 0.25$	$0.16 \times 0.16 \times 0.04$	$0.25 \times 0.15 \times 0.10$	$0.25 \times 0.15 \times 0.05$
Crystal system	tetragonal	triclinic	monoclinic	triclinic
Space group	$I4_1/a$ (no. 88)	$P\bar{1}$(no. 2)	$P2_1/c$ (no. 14)	$P\bar{1}$ (no. 2)
Unit cell dimensions				
a (Å)	24.755(2)	7.5336(8)	8.096(8)	8.2936(17)
b (Å)	24.755(2)	10.2937(10)	11.123(3)	10.6015(17)
c (Å)	9.439(2)	11.6774(7)	15.988(8)	11.3430(15)
α (°)	90	108.855(7)	90	105.504(17)
β (°)	90	101.405(8)	103.92(8)	101.881(19)
γ (°)	90	91.475(11)	90	96.91(2)
V (Å^3)	5784.3(15)	836.12(13)	1397.5(5)	924.0(3)
Z	16	2	4	2
D_{calc} (g cm^{-3})	1.562	1.674	1.639	2.038
μ (mm^{-1})	1.494	4.598	1.720	7.982
θ Range (°)	2.31–27.98	4.10–62.16	1.31–27.48	2.34–30.41
Index ranges	$-32 \le h \le 0$, $0 \le k \le 32$, $0 \le l \le 12$	$-8 \le h \le 8$, $-11 \le k \le 11$, $-13 \le l \le 0$	$0 \le h \le 10$, $-14 \le k \le 14$, $-20 \le l \le 20$	$0 \le h \le 11$, $-15 \le k \le 14$, $-16 \le l \le 15$
Max/min transmissions	0.977/0.847	0.960/0.820	1.000/0.915	0.982/0.465
Reflections collected	3642	2804	3198	5918
Independent reflections [R_{int}]	3477 (0.0674)	2654 (0.1037)	2293 (0.0235)	5569 (0.0426)
Data/parameters	3477/181	2654/226	2293/224	5569/220
Final R indices [$I > 2\sigma(I)$]	$R_1 = 0.0422$, $wR_2 = 0.0849$	$R_1 = 0.0683$, $wR_2 = 0.1452$	$R_1 = 0.0387$, $wR_2 = 0.0903$	$R_1 = 0.0424$, $wR_2 = 0.0791$
R indices (all data)	$R_1 = 0.1829$, $wR_2 = 0.1112$	$R_1 = 0.2668$, $wR_2 = 0.2057$	$R_1 = 0.0661$, $wR_2 = 0.1203$	$R_1 = 0.1313$, $wR_2 = 0.0979$
Goodness-of-fit on F^2	0.957	0.924	1.188	1.011
Largest difference peak and hole (e Å^{-3})	0.311 and −0.496	0.447 and −0.362	0.554 and −0.986	1.180 and −2.217

Table 2
Selected bond distances (Å) for [Ni(Am4DM)(OAc)], **1**, [Ni(Am4DM)(CH_3CN)]ClO_4, **2**, [Cu(Am4DM)(OAc)], **3**, and [Pt(Am4DM)(DMSO)]$Cl\cdot 2H_2O$, **4**

Bond	1	2	3	4
M–N(11)	1.923(3)	1.900(9)	2.058(4)	2.077(5)
M–N(12)	1.829(3)	1.812(7)	1.918(3)	1.964(5)
M–S(1)	2.145(1)	2.138(3)	2.274(2)	2.259(2)
M–O(11)[N(1),S(2)]	1.874(3)	1.842(8)	1.923(3)	2.227(2)
S(1)–C(17)	1.752(4)	1.778(11)	1.746(3)	1.765(7)
C(16)–N(12)	1.305(4)	1.311(12)	1.305(4)	1.306(8)
N(12)–N(13)	1.388(4)	1.373(10)	1.385(4)	1.399(7)
N(13)–C(17)	1.319(5)	1.302(12)	1.321(4)	1.312(8)
C(17)–N(14)	1.345(5)	1.337(12)	1.356(4)	1.349(9)
C(16)–N(15)	1.343(5)	1.354(13)	1.329(5)	1.307(8)
C(11)–O(11)	1.285(5)		1.276(5)	1.464(5) [a]
C(11)–O(12)	1.227(5)		1.233(6)	

[a] S(2)–O(20).

anionic oxygen donor, $[OAc]^-$, compared with a neutral nitrogen donor (i.e. CH_3CN). All of the bonds to nickel(II) by Am4DM are shorter in [Ni(Am4DM)(CH_3CN)]ClO_4 compared with [Ni(Am4DM)(OAc)] and S(1)–C(17) and C(16)–N(12) are both marginally longer. The stronger coordination by Am4DM in [Ni(Am4DM)(CH_3CN)]ClO_4 compared

Table 3
Selected bond angles (°) for [Ni(Am4DM)(OAc)], **1**, [Ni(Am4DM)(CH_3CN)]ClO_4, **2**, [Cu(Am4DM)(OAc)], **3**, and [Pt(Am4DM)(DMSO)]$Cl\cdot 2H_2O$, **4**

Bond	1	2	3	4
S(1)–M–N(12)	86.36(10)	85.9(3)	83.50(10)	84.07(15)
S(1)–M–N(11)	169.83(11)	170.5(3)	159.97(9)	163.45(15)
S(1)–M–O(11)-[N(1),S(2)]	94.03(9)	92.7(3)	99.97(10)	94.00(7)
N(12)–M–N(11)	83.66(14)	84.7(4)	80.03(13)	79.4(2)
N(12)–M–O(11)-[N(1),S(2)]	179.51(14)	176.3(4)	176.52(11)	178.03(16)
N(11)–M–O(11)-[N(1),S(2)]	95.95(14)	96.7(4)	96.50(14)	102.53(16)
M–S(1)–C(17)	96.03(14)	95.2(4)	95.25(12)	96.0(2)
M–N(12)–C(16)	117.7(3)	117.3(7)	119.3(2)	119.7(4)
M–N(12)–N(13)	125.4(2)	127.7(7)	125.2(2)	123.5(4)
N(15)–C(16)–N(12)	123.6(4)	124.5(10)	123.6(3)	124.8(6)
C(15)–C(16)–N(12)	113.4(4)	113.3(10)	114.0(3)	113.5(6)
C(16)–N(12)–N(13)	116.7(3)	115.1(8)	115.2(3)	116.7(6)
N(12)–N(13)–C(17)	109.9(3)	108.5(9)	110.9(3)	112.1(6)
N(13)–C(17)–N(14)	118.9(4)	120.9(10)	115.9(3)	118.0(7)
N(13)–C(17)–S(1)	122.1(3)	122.6(8)	124.3(3)	124.2(5)
N(14)–C(17)–S(1)	119.0(3)	116.5(9)	119.9(3)	117.8(5)
Pt(1)–S(2)–O(20)				118.7(2)
Pt(1)–S(2)–C(21)				111.1(3)
Pt(1)–S(2)–C(22)				109.4(3)
M–O(11)[N(1)]–(C1)	119.0(3)	177.5(10)	116.7(3)	

Table 4
Hydrogen bonding interactions for [Ni(Am4DM)(OAc)], **1**, [Ni(Am4DM)(CH_3CN)]ClO_4, **2**, [Cu(Am4DM)(OAc)], **3**, and [Pt(Am4DM)(DMSO)]$Cl\cdot 2H_2O$, **4**

Compound	D–H···A	d(D–H)	d(H···A)	d(D···A)	∠ (DHA)
1 [a]	N(15)–H(15A)···S(1)#2	0.86	3.27	3.953(4)	137.9
	N(15)–H(15B)···O(12)#1	0.86	2.05	2.800(4)	145.5
2 [b]	N(15)–H(15A)···O(11)#1	1.15(10)	2.14(11)	3.231(13)	158(7)
	N(15)–H(15B)···O(12)#2	0.72(10)	2.37(10)	3.052(12)	160(13)
3 [c]	N(15)–H(15B)···O(12)#1	0.71(4)	2.20(4)	2.885(7)	162(4)
	C(12)–H(12)···O(12)#1	0.96(4)	2.73(4)	3.627(6)	154(3)
	C(13)–H(13)···O(12)#2	0.97(5)	2.76(5)	3.394(5)	123(3)
	C(14)–H(14)···S(1)#3	1.00(5)	2.91(5)	3.587(6)	126(4)
4 [d]	N(15)–H(15A)···O(1)#1	0.86	2.22	3.000(9)	150.6
	N(15)–H(15B)···Cl(1)#1	0.86	2.46	3.222(6)	148.0
	O(1)–H(1A)···O(2)#2	0.85(9)	2.30(9)	2.889(13)	126(8)
	O(1)–(H1B)···O(20)#3	0.87(9)	2.62(9)	3.057(9)	112(7)
	O(2)–H(2A)···Cl(1)#2	0.56(10)	2.69(10)	3.251(7)	175(17)
	O(2)–H(2B)···Cl(1)#4	0.99(9)	2.27(9)	3.251(10)	169(7)

[a] Symmetry transformations used to generate equivalent atoms; #1: $-x+1/2$, $-y$, $-z+7/4$; #2: $-y+1/2$, $x-1/2$, $-z+3/2$.
[b] Symmetry transformations used to generate equivalent atoms; #1: $-x+1$, $-y+2$, $-z+2$; #2; x, y, $z-1$.
[c] Symmetry transformations used to generate equivalent atoms; #1: $-x+1$, $-y$, $-z+2$; #2: $x+1/2$, $-y+1/2$, $z+1/2$; #3: $x+1/2$, $-y+1/2$, $z+1/2$.
[d] Symmetry transformations used to generate equivalent atoms; #1: $-x+1$, $-y$, $-z$; #2: $-x+1$, $-y+1$, $-z+1$; #3: $-x+1$, $-y$, $-z+1$; #4: $x-1$, y, z.

with [Ni(Am4DM)(OAc)] is due to weaker coordination by the *sp* hybridized N of a neutral molecule, reduced steric requirement of CH_3CN compared with $[OAc]^-$, and increased charge on Ni in the cationic center, which would be enhanced by the ability of CH_3CN to serve as an acceptor of π-electron density. The Ni–N bond is shorter for the sp^2 hybridized imine nitrogen than the *sp* hybridized acetonitrile nitrogen, which is substantially shorter than the Ni–N(pyridine) bond. The bond angles around nickel(II) for the two complexes do not differ significantly.

The hydrogen atoms on N(15) interact with oxygen atoms of two different perchlorate ions, once again demonstrating that hydrogen bonding by these two hydrogen atoms is a common feature of the 2-pyridine-formamide thiosemicarbazones [5–12]. The donor atom mean plane about Ni(1) has greater deviation than found for [Ni(Am4DM)(OAc)] and Ni(1) is 0.014 (5) Å from the plane. The thiosemicarbazone moiety is at a similar angle to the coordination plane in [Ni(Am4DM)(CH_3CN)]ClO_4 and [Ni(Am4DM)(OAc)].

3.1.3. Structure of [Cu(Am4DM)OAc]

All metal–ligand bond distances in [Cu(Am4DM)(OAc)], including the acetato ligand, are longer than the analogous bonds in [Ni(Am4DM)(OAc)]; the bond with sulfur has the greatest difference, Table 2. However, the bond distances of the thiosemicarbazone moiety in the two complexes are not significantly different. The larger copper(II) ion forces the N(11)–

Table 5
Rms planes for [Ni(Am4DM)(OAc)], **1**, [Ni(Am4DM)(CH_3CN)]ClO_4, **2**, [Cu(Am4DM)(OAc)], **3**, and [Pt(Am4DM)(DMSO)]$Cl\cdot 2H_2O$, **4**.

Compound	Plane	Rms dev.	Largest dev.	∠ with previous plane
1	O(11)–O(12)–C(12)	0.0000		
	S(1)–N(12)–N(11)–O(11)	0.0149	N(12), 0.016(2)	77.0(1)
	C(16)–N(12)–N(13)–C(17)–S(1)–N(14)	0.0183	N(13), 0.029(3)	3.2 (2)
	N(11)–C(11)–C(12)–C(13)–C(14)–C(15)	0.0021	C(11), 0.004(3)	1.0(2)
2	S(1)–N(12)–N(11)–N(1)	0.0414	N(12), 0.045(4)	
	C(16)–N(12)–N(13)–C(17)–S(1)–N(14)	0.0168	N(12), 0.025(7)	3.8(3)
	N(11)–C(11)–C(12)–C(13)–C(14)–C(15)	0.0096	N(11), 0.013(7)	2.4(4)
3	N(11)–C(11)–C(12)–C(13)–C(14)–C(15)	0.0118	C(14), 0.018(3)	
	C(16)–N(12)–N(13)–C(17)–S(1)–N(14)	0.0985	C(16), 0.145(2)	12.2(2)
	N(11)–N(12)–S(1)–O(11)	0.1054	N(12), 0.122(2)	4.6(1)
	O(11)–C(11)–O(12)–C(12)	0.0009	C(11), 0.002(3)	89.0(1)
4	N(11)–N(12)–S(1)–S(2)	0.0039	N(12), 0.005(3)	
	C(16)–N(12)–N(13)–C(17)–S(1)–N(14)	0.0110	N(13), 0.020(6)	0.8(2)
	N(11)–C(11)–C(12)–C(13)–C(14)–C(15)	0.0084	C(15), 0.012(5)	0.5(3)

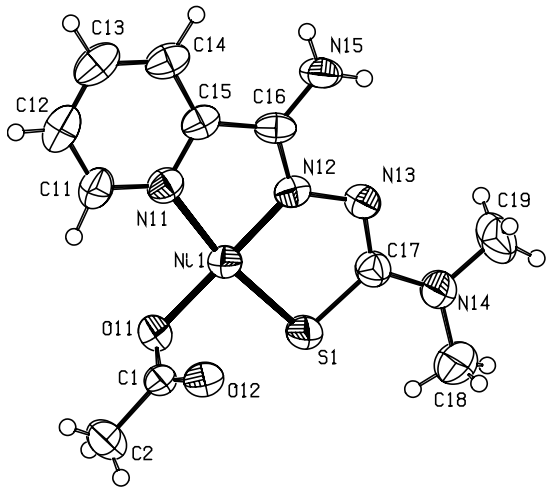

Fig. 2. The [Ni(Am4DM)(OAc)] molecule with the numbering scheme of the non-hydrogen atoms. Displacement ellipsoids are plotted at the 50% probability level and H atoms are presented as spheres of arbitrary radii.

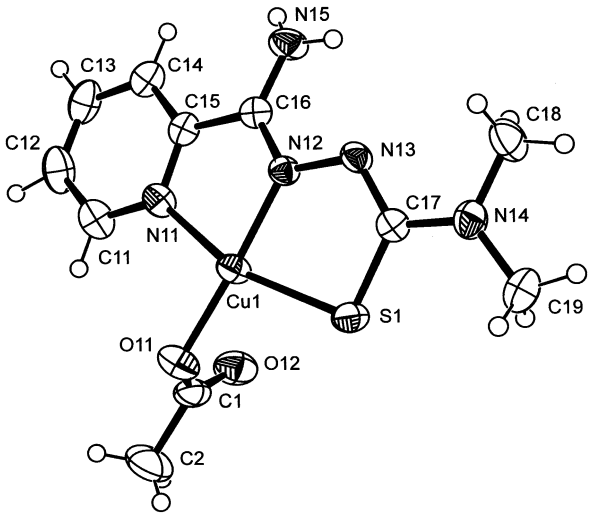

Fig. 4. Two unique molecules of [Cu(Am4DM)(OAc)]. The non-hydrogen atoms are drawn at 50% probability contours of the thermal motion, while the hydrogen atoms have an arbitrary size.

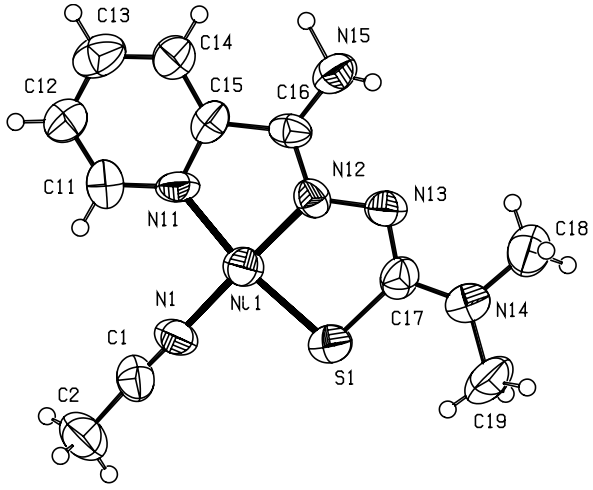

Fig. 3. The [Ni(Am4DM)(MeCN)] molecule with the numbering scheme of the non-hydrogen atoms. Displacement ellipsoids are plotted at the 50% probability level and H atoms are presented as spheres of arbitrary radii.

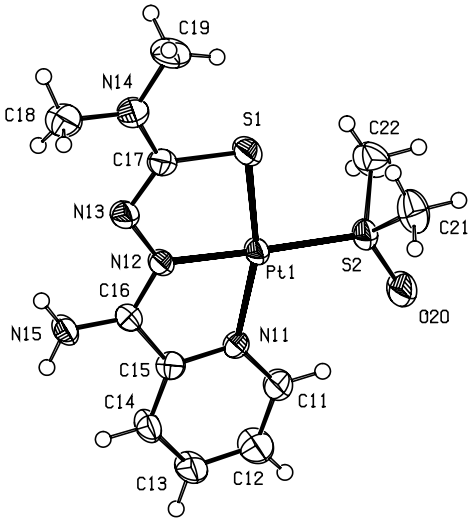

Fig. 5. The [Pt(Am4DM)(DMSO)]Cl molecule with the numbering scheme of the non-hydrogen atoms. Displacement ellipsoids are plotted at the 50% probability level and H atoms are presented as spheres of arbitrary radii.

M–S(1) angle to be approximately 10° less in [Cu(Am4DM)(OAc)] compared with [Ni(Am4DM)(OAc)]. The other angles about the two metal centers are more similar and the angles within the thiosemicarbazone moiety are essentially the same in the two complexes. Also, the bond distances of [Cu(Am4DM)(OAc)] are comparable to binuclear [Cu(Amheximi)]$_2$[succinate], where Amhexim is the anion of 2-pyridineformamide [11], which appears to have '4+1' coordination with the second oxygen of the carboxylato function 2.863(3) Å from the Cu atom. In [Cu(Am4DM)(OAc)] the second oxygen of the acetato ligand is at a distance of approximately 2.92 from Cu(1) and is involved in intermolecular hydrogen bonding (vide infra) as found for [Cu(Amhexim)]$_2$[succinate]. Therefore, the coordination for [Cu(Am4DM)(OAc)] can also be considered to be '4+1'.

The strongest hydrogen bonding interaction for [Cu(Am4DM)(OAc)], like [Ni(Am4DM)(OAc)], involves a N(15)H$_2$ hydrogen, H(15B), interacting with the non-coordinated oxygen of the acetato group, O(12), in a neighboring molecule. The H(15B)···O12 distance is somewhat longer, 2.20(4) Å, than in [Ni(Am4DM)(OAc)], 2.05 Å. In addition, there are some weaker interactions by C–H's with the weakly coordinated acetato oxygen atoms and coordinated sulfur atoms of neighboring molecules; the H···X distances are between

2.70 and 3.00 Å. The four donor atoms, N(11)–N(12)–S(1)–O(11), in [Cu(Am4DM)(OAc)] are much more distorted from a plane than in [Ni(Am4DM)(OAc)] and copper(II) is 0.105 (1) Å from the plane toward O(12). The acetato function makes an angle of approximately 89° with the coordination plane compared with approximately 77° for [Ni(Am4DM)(OAc)].

3.1.4. Structure of [Pt(Am4DM)DMSO]Cl·2H$_2$O

Dissolution of [Pt(Am4DM)Cl]·2H$_2$O in DMSO produced diffraction-quality crystals of [Pt(Am4DM)(DMSO)]Cl. This is experimental proof of the facile solvolysis in which the Cl^- ion is displaced from the coordination sphere of the platinum atom:

$$[Pt(L)Cl] + DMSO \rightleftarrows [Pt(L)(DMSO)]^+ + Cl^-$$

usually confirmed by NMR [21].

Like the preceding complexes, coordination of tridentate Am4DM is via the pyridine nitrogen, the imine nitrogen, and the thiolato sulfur atoms and the DSMO molecule coordinates via the sulfur atom. The platinum(II)–nitrogen bond distances are longer than the analogous copper(II)–nitrogen distances in [Cu(Am4DM)(OAc)], but Pt–S for Am4DM is shorter than Cu–S presumably due to the softer Pt(II) center. The N(11)–Pt(1)–S(1) angle is in between that of [Ni(Am4DM)(OAc)] and [Cu(Am4DM)(OAc)]. The most noticeable difference in angles of the coordinate bonds between [Pt(Am4DM)(DMSO)]Cl and the other complexes of this study is that the N(11)–Pt(1)–S(2) angle, 102.53(16)°, is larger than approximately 96° for N(11)–M–O(11)(N1). The angles made by the functions coordinating to Pt (i.e. Pt(1)–S(1)–C(17), Pt(1)–N(12)–C(16), etc.) and the angles within the thiosemicarbazone moiety are essentially the same as for the other complexes of this study.

There is extensive hydrogen bonding to the DMSO oxygen by a water molecule, to the chloride anion by the second water molecule and between the water molecules, Table 4. The amide NH_2 hydrogen atoms interact with a hydrate water oxygen and the chloride ion, but not with the DMSO oxygen. The coordination sphere [i.e. N(11)–N(12)–S(1)–S(2)] has the smallest deviation from planarity for these complexes, and the Pt center is 0.012(2) Å from the mean plane. The mean planes of the thiosemicarbazone moiety and pyridine ring are essentially co-planar with the coordination plane.

3.2. Characterization of the complexes

In [Fe(Am4DM)$_2$]ClO$_4$ and [Co(Am4DM)$_2$]ClO$_4$, each Am4DM anion is coordinated as a NNS tridentate ligand, and the complexes have a meridonal arrangement as found for the analogous complexes of 2-pyridineformamide *N*(4)-methylthiosemicarbazone, [Fe(Am4M)$_2$]ClO$_4$ and [Co(Am4M)$_2$]ClO$_4$ [7]. The meridonal arrangement results from the necessary planarity of the conjugated anionic ligands and has been found for 2-substituted pyridine bis(thiosemicarbazonato) iron(III), cobalt(III) and nickel(II) [7,23–28] complexes. The dark brown [Fe(Am4DM)$_2$]ClO$_4$ is low spin, $\mu =$ 1.9 B.M., in agreement with previously studied iron(III) complexes with two heterocyclic thiosemicarbazone ligands. Loss of hydrogen from the thiosemicarbazone moiety and coordination in [Fe(Am4DM)$_2$]ClO$_4$ results in ν(CN) decreasing 14 cm^{-1}, ν(CS) decreasing 87 cm^{-1} and ν(py) increasing 21 cm^{-1}, consistent with coordination of the pyridine and imine nitrogen atoms and the thiolato sulfur atom. Also, the spectrum shows strong bands for ν_3(ClO$_4$) and ν_4(ClO$_4$) at 1056 and 622 cm^{-1} for the perchlorate ion. Although a rhombic ESR spectrum is common for low spin bis(heterocyclic thiosemicarbazone)iron(III) complexes [7,11,23,26], [Fe(Am4DM)$_2$]ClO$_4$ has a single broad line suggesting considerable interaction between iron(III) centers.

Oxidation to cobalt(III) occurs during preparation of complexes of heterocyclic thiosemicarbazones using cobalt(II) salts with weakly coordinating anions [25,28]. The mechanism of this oxidation has not been proposed, but it is known that preparations with the analogous semicarbazones do not produce cobalt(III) salts [26]. Thus, [Co(Am4DM)$_2$]ClO$_4$ is diamagnetic and has infrared bands similar to those of [Fe(Am4DM)$_2$]ClO$_4$. The solid state electronic spectrum has absorption bands consistent with approximately octahedral cobalt(III), and we suggest the following assignments: $^1A_{1g} \rightarrow {}^1T_{1g}$, 21 960 cm^{-1}; $^1A_{1g} \rightarrow {}^1T_{2g}$, 26 000 cm^{-1}; $^1A_{1g} \rightarrow {}^3T_{1g}$, 6710 cm^{-1} and $^1A_{1g} \rightarrow {}^3T_{2g}$, 15 130 cm^{-1}. Assignment of the two higher energy bands is complicated by overlap with the more intense intraligand and charge transfer bands. However, these assigned energies allow calculation of $Dq = 2.420$ cm^{-1} and $B = 653$ cm^{-1}, which indicate that Am4DM provides more covalent bonding and a stronger ligand field than Am4M in [Co(Am4M)$_2$]ClO$_4$, $Dq = 2.220$ cm^{-1} and $B = 820$ cm^{-1} [7].

Ni(Am4DM)(OAc)] was isolated from its preparative mixture as the monohydrate, is diamagnetic and has a molar conductivity consistent with a non-electrolyte. The mass spectrum of [Ni(Am4DM)(OAc)] shows the cluster of ions centered at *m*/*z* 339 (i.e. [M−1]) and fragmentation ions are observed at M−32, M−51, M−59, and M−107 suggesting loss of S (or possibly O_2), for the first fragment and loss of acetate ion for the third fragment and largest fragmentation peak.

The IR bands at 1594 and 1564 cm^{-1} are primarily due to ν(CN) with the former assigned to the N(13)–C(17) formal double bond formed on coordination and the latter to the C(16)–N(12) bond which is lower in energy by 18 cm^{-1} than the analogous bond in HAm4DM. The thioamide IV band is shifted from above 800 cm^{-1} in the spectrum of HAm4DM to a

shoulder at 745 cm^{-1} consistent with the reduction in the C–S bond order and coordination to the nickel(II) center. We assign ν(NiN, imine), ν(NiO) and ν(NiS) at 480, 384 and 369 cm^{-1}, respectively, which are similar to assignments of previously studied 2-pyridineformamde N(4)-substituted thiosemicarbazone complexes prepared with nickel(II) acetate [7,9,11]. The solid state electronic spectrum of [Ni(Am4DM)(OAc)] shows a $n \rightarrow \pi^*$ band, which is a combination of the transitions due to imine functions, the thiol function and the pyridine ring, at 29 260 cm^{-1}, a band at 23 620 cm^{-1} due to S→Ni(II) charge transfer transition and the following d→d bands: $^1A_{1g} \rightarrow {}^1B_{1g}$. 21 190 cm^{-1}; $\rightarrow {}^1A_{2g}$, 19 380 cm^{-1} and $\rightarrow {}^1E_g$, 16 290 cm^{-1}, consistent with its planar stereochemistry.

The spectroscopic and magnetic data in $[Ni(HAm4DM)_2](ClO_4)_2$ and $[Ni(HAm4DM)_2](NO_3)_2$ are similar. The IR spectra of both complexes exhibit three bands between 3440–3370, 3350–3280 and 3250–3190 due to the presence of the amida and imino groups and shows ν(CN) at 1561 cm^{-1}, ν(CS) at 854 cm^{-1}, ν(Ni–N) approximately 475 cm^{-1} and ν(NiS) approximately 360 cm^{-1} consistent with coordination of the imine nitrogen and thione sulfur atoms of both ligands. The ν_3 and ν_4 absorptions of the ionic perchlorate are present as strong peaks at 1108 and 627 cm^{-1}, respectively. The latter band makes it difficult to assign the out-of-plane ν(py) band often used to indicate coordination of pyridine nitrogen atoms. In $[Ni(HAm4DM)_2](NO_3)_2$ two bands appearing at 1384 and 839 cm^{-1} are assigned to ν_3 and ν_4 vibrations of the ionic nitrate whereas a weak band at 642 cm^{-1} is assigned to ν(py) consistent with coordination of the pyridine nitrogen atom. The solid state electronic spectra have absorption bands at 11 660–11 723 and 17 065–17 240 cm^{-1}, but assignment as $^3A_{2g} \rightarrow {}^3T_{1g}$(P) and $\rightarrow {}^3T_{1g}$(F), respectively, and attempts to calculate ligand field parameters indicate that the complex are significantly distorted from octahedral symmetry.

The molar conductivity of $[Ni(HAm4DM)_2]X_2$ (10^{-3} M in DMF) is 190 and 154 Ω^{-1} cm^2 mol^{-1} for perchlorate and nitrate, respectively, consistent with a 1:2 electrolyte [22]. The M−1 fragment is not present in the mass spectra of the complexes; the heaviest fragmentation cluster is at [M−41]. Also present are fragment clusters at [M−201] and [M−397]. The former cluster probably represents loss of the two anions and formation of $[Ni(Am4DM)_2]$.

The mass spectra of [Pd(Am4DM)Cl] and $[Pt(Am4DM)Cl]\cdot 2H_2O$ show signals for the molecular ion M^+ at m/z 363 and 503, respectively. Both complexes are diamagnetic and a non-electrolyte. In the IR spectra the ν(NH) vibrations are observed around 3470–3430 and 3360–3280 cm^{-1}, but the spectra do no exhibit the stretching vibration corresponding to ν(NH) (hydrazine) and substantiates the deprotonation of HAm4DM [12]. Medium intensity infrared bands for ν(M–N, imine), ν(M–S) and ν(M–Cl) are assigned at 484, 381 and 344 cm^{-1} for the palladium(II) complex, and at 465, 395 and 333 cm^{-1} for the platinum(II) complex, respectively. The ^{1}H NMR spectra shows a doublet of doublets at 8.80 ppm assignable to C(11)H (Fig. 5) and the amide group hydrogen atoms at 7.37 ppm. The ^{13}C NMR spectrum shows C(S) at 177.3 ppm and the imine carbon at 150.5 ppm in [Pd(Am4DM)Cl] and 176.8 ppm and the imine carbon at 151.9 ppm in $[Pt(Am4DM)Cl]\cdot 2H_2O$, and the ^{195}Pt resonance is at −31 050 ppm.

[Cu(Am4DM)(OAc)] is a non-electrolyte with a magnetic susceptibility of 1.8 B.M. The composite $n \rightarrow \pi^*$ band is at 32 820 cm^{-1}, the S→Cu(II) charge transfer band at 23 750 cm^{-1} and a broad composite d→d band at 16 770 cm^{-1}. The ESR spectrum has a slight rhombic character with $g_1 = 2.166$, $g_2 = 2.059$ and $g_3 = 2.029$ with $g_{av} = 2.085$ indicative of a $d_{x^2-y^2}$ (or d_{xy}) ground state. [Cu(Ampip)OAc] has $g_1 = 2.188$, $g_2 = 2.059$ and $g_3 = 2.034$ with $g_{av} = 2.093$ suggesting marginally more covalent bonding in [Cu(Am4DM)(OAc)].

Reaction of HAm4DM with copper(II) chloride yields $[Cu(HAm4DM)Cl_2]$, but when a small amount of triethylamine is added to the reaction mixture [Cu(Am4DM)Cl] is produced. Both brown solids have normal magnetic moments (i.e. ca. 1.8 B.M.) for monomeric copper(II) complexes. $[Cu(HAmpip)Cl_2]$ has d→d bands at 19 400 and 14 980 cm^{-1} which are both higher in energy than 17 520 and 14 010 cm^{-1} found for $[Cu(HAmpip)Cl_2]$ [8]. $[Cu(HAmpip)Cl_2]$ is a distorted square pyramid with one chloro ligand in the apical position, and based on the energies of the d→d bands $[Cu(HAm4DM)Cl_2]$ is a less distorted square pyramid probably due to lesser space requirements of Am4DM compared with Ampip. The powder ESR spectrum of $[Cu(HAm4DM)Cl_2]$ is consistent with a $d_{x^2-y^2}$ ground state and has a slight rhombic appearance consistent with unequal coordination distances about the basal plane; the g-values, 2.204, 2.061 and 2.052, which average 2.106, are all higher than found for $[Cu(HAmpip)Cl_2]$, 2.158, 2.046, 2.036 and an average of 2.080. The higher g-values for $[Cu(Am4DM)Cl_2]$ are consistent with stronger bonding of the apical chloro ligand and less distortion of the square pyramid.

[Cu(Am4DM)Cl], like [Cu(Am4DM)(OAc)], is a planar complex with a d→d composite band at 16 460 cm^{-1}, which is lower than 16 770 cm^{-1} found for [Cu(Am4DM)OAc], indicating weaker coordination by the chloro ligand compared with the acetato ligand. As is often the situation in the ESR spectra for four-coordinate complexes of copper(II) with two or more soft donor atoms (i.e. S, Cl, Br etc.), the highest g-value feature is obscured by the rest of the spectrum of [Cu(Am4DM)Cl].

4. Conclusion

Our results again indicate that thiosemicarbazones attached to 2-pyridineformamide coordinate more strongly to metal ions than the analogous complexes prepared from 2-formylpyridine, 2-acetylpyridine and 2-benzoylpyridine. Thus, this series of thiosemicarbazones, because of stronger bonding to metal ions may be more active and their metal complexes may possess greater selectivity because of this stronger coordination.

5. Supplementary material

Crystallographic data for the structures reported in this paper (excluding structure factors) have been deposited with the Cambridge Crystallographic Data Centre as Supplementary Publication No. CCDC-189171 [Ni(Am4DM)OAc]; CCDC-189172, [Ni(Am4DM)(CH_3CN)]ClO_4; CCDC-174188, [Cu-(Am4DM)OAc] and CCDC-189173, [Pt(Am4DM)-DMSO]$Cl\cdot 2H_2O$ Copies of the data can be obtained free of charge on application to CCDC, 12 Union Road, Cambridge CB2 1EZ, UK (fax: +44-1223-336033; e-mail: deposit@ccdc.cam.ac.uk or www: http://www.ccdc.cam.ac.uk).

Acknowledgements

Acknowledgement is made to the Donors of the Petroleum Research Fund, administered by the American Chemical Society, for the partial support of this research.

References

[1] D.X. West, C.E. Ooms, J.S. Saleda, H. Gebremedhin, A.E. Liberta, Transition Met. Chem. 19 (1994) 553 (and references therein).
[2] D.X. West, H. Gebremedhin, R.J. Butcher, J.P. Jasinski, A.E. Liberta, Polyhedron 12 (1993) 2489 (and references therein).
[3] D.X. West, J.S. Ives, J. Krejci, M.M. Salberg, T.L. Zumbahlen, G.A. Bain, A.E. Liberta, J. Valdés-Martínez, S. Hernández-Ortega, R.A. Toscano, Polyhedron 14 (1995) 2189.
[4] (a) M.C. Miller, C.N. Stineman, J.R. Vance, D.X. West, I.H. Hall, Anticancer Res. 18 (1998) 4131;
(b) M.C. Miller, C.N. Stineman, J.R. Vance, D.X. West, I.H. Hall, Appl. Organomet. Chem. 13 (1999) 9.
[5] A. Castiñeiras, I. Garcia, E. Bermejo, D.X. West, Z. Naturforsch. 55 (2000) 511.
[6] A. Castiñeiras, I. Garcia, E. Bermejo, D.X. West, Polyhedron 19 (2000) 1873.
[7] D.X. West, J.K. Swearingen, J. Valdés-Martínez, S. Hernández-Ortega, A.K. El-Sawaf, F. van Meurs, A. Castiñeiras, I. Garcia, E. Bermejo, Polyhedron 18 (1999) 2919.
[8] D.X. West, J.K. Swearingen, A.K. El-Sawaf, Transition Met. Chem. 25 (2000) 87.
[9] A. Castiñeiras, I. Garcia, E. Bermejo, K.A. Ketcham, D.X. West, A.K. El-Sawaf, Z. Anorg. Allg. Chem. 628 (2002) 492.
[10] K.A. Ketcham, J.K. Swearingen, A. Castiñeiras, I. Garcia, E. Bermejo, D.X. West, Polyhedron 20 (2001) 3265.
[11] K.A. Ketcham, I. Garcia, E. Bermejo, J.K. Swearingen, A. Castiñeiras, D.X. West, Z. Anorg. Allg. Chem. 628 (2002) 409.
[12] E. Bermejo, A. Castiñeiras, L.M. Fostiak, I. Garcia, A.L. Llamas, J.K. Swearingen, D.X. West, Z. Naturforsch. 56 (2001) 1297.
[13] J.P. Scovill, Phosphorus, Sulfur Silicon 60 (1991) 15.
[14] J. van Koningsbruggen, J.G. Haasnoot, R.A.G. De Graaff, J. Reedijk, Inorg. Chim. Acta 234 (1995) 87.
[15] G.A. Bain, D.X. West, J. Krecji, J. Valdés-Martínez, S. Hernández-Ortega, R.A. Toscano, Polyhedron 16 (1997) 855.
[16] M. Kretschmar, GENHKL Program for the Reduction of CAD4 Diffractometer Data, University of Tübingen, Germany, 1997.
[17] G.M. Sheldrick, Acta Crystallogr., Sect. A 46 (1968) 467.
[18] G.M. Sheldrick, SHELXL-97. Program for the Refinement of Crystal Structures, University of Göttingen, Germany, 1997.
[19] International Tables for Crystallography, vol. C, Kluwer Academic Publishers, Dordrecht, The Netherlands, 1995.
[20] A.L. Spek, PLATON. A Multipurpose Crystallographic Tool, University of Utrecht, The Netherlands, 2001.
[21] K.R. Koch, J. Coord. Chem. 22 (1991) 289.
[22] W.J. Geary, Coord. Chem. Rev. 7 (1971) 81.
[23] D.X. West, P. Ahrweiler, G. Ertem, J.P. Scovill, D.L. Klayman, J.L. Flippen-Anderson, R. Gilardi, C. George, L.K. Pannell, Transition Met. Chem. 10 (1985) 264.
[24] A. Castiñeiras, H. Gebremedhin, T.J. Romack, D.X. West, Inorg. Chim. Acta 216 (1994) 229.
[25] C. Maichle, A. Castiñeiras, R. Carballo, H. Gebremedhin, M.A. Lockwood, C.E. Ooms, T.J. Romack, D.X. West, Transition Met. Chem. 20 (1995) 228.
[26] D.X. West, I.S. Billeh, G.A. Bain, J. Valdés-Martínez, K.H. Ebert, S. Hernández-Ortega, Transition Met. Chem. 21 (1996) 572.
[27] D.X. West, M.A. Lockwood, A. Castiñeiras, Transition Met. Chem. 22 (1997) 447.
[28] D.X. West, B.L. Mokijewski, H. Gebremedhin, T.J. Romack, Transition Met. Chem. 17 (1992) 384.